Proceedings of the 3rd International Symposium on Uncertainty Quantification and Stochastic Modeling
D.A. Rade; A. M. G. Lima (Editors), ABCM, Maresias, SP, Brazil, February 15-19, 2016

Sensitivity analysis of the dynamic characteristics of thrust bearings

Gregory Bregion Daniel[1], Leonardo Carpinetti Vieira[1], and Katia Lucchesi Cavalca[1]

[1] Laboratory of Rotating Machinery, Faculty of Mechanical Engineering

University of Campinas, Mendeleyev 200, Campinas – SP, 13083-860

Abstract: The hydrodynamic bearing has an important role in rotating machinery, because its characteristics can directly affect the dynamic behavior of the rotor. On other hand, the behavior of the thrust bearing depends on several parameters, namely, clearance, oil film temperature (or viscosity), oil film minimum thickness and loading. Certainly relative velocity is also an important parameter, however in this paper the focus is mainly on the oil film thickness and the experimental validation of the dynamic coefficient of stiffness. To reproduce the complete rotating system, an accurate modeling of the bearings is, then, mandatory. Here, a turbocharger thrust bearing is represented by a thermohydrodynamic model and inserted in the numerical model of the turbocharger rotor as equivalent dynamic coefficients of stiffness and damping. To proceed with the experimental validation, an experimental set up is assembled in order to measure axial load and displacement of the shaft for several rotation speeds. The numerical simulation of the experimental set up is accomplished and the results are compared. However, uncertainties related to the assembling and, mainly, to some measurements are found to propagate up to the final estimation of the oil film thickness and, consequently, the stiffness coefficient. Facing this problem, a statistical analysis of the experimental results is fundamental to establish a confidence bound of the parameters estimation. The confidence limits conditions were, then, numerically simulated and interesting results about the parameters sensitivity are reached. At this point, the experimental validation of the bearing model is presented in terms of mean value and standard deviation, considering Gaussian distribution for the uncertainties.

Keywords: thrust bearings, stiffness coefficients, experimental validation, measurements uncertainties.

INTRODUCTION

The industry demand of high performance and downsizing of machines and equipments claims for devices with even more high rotation speeds and severe loading. Such equipments can be found in several applications as power generation plants, power units, automotive industry and so on. If flux machines are involved in the process, axial displacements and efforts are present in the dynamic of the system. Consequently, hydrodynamically lubricated thrust bearings should be employed in such equipments. The behavior of the thrust bearing depends on several parameters, namely, clearance, oil film temperature (or viscosity), oil film minimum thickness and loading. Certainly relative velocity is also an important parameter, however in this paper the focus is mainly on the oil film thickness and the experimental validation of the dynamic coefficient of stiffness. To reproduce the complete rotating system, an accurate modeling of the bearings is, then, mandatory.

The lubricated system response to the external excitation is a crucial factor on the system design due to the specific dynamic characteristics necessary to guarantee the high performance of the system. At this point, a numerical model to evaluate the system behavior when hydrodynamic thrust bearings are applied under high rotation speeds needs to take into account then thermal effects on the fluid film. The present work presents a thermohydrodynamic (THD) model, and a test bench, specifically adapted to analyze the axial behavior of a shaft assembled on thrust bearings and subjected to high rotation frequencies. The equivalent axial direct stiffness coefficient of the fluid film of the thrust bearing is estimated numerically and experimentally.

However, uncertainties related to the assembling and, mainly, to some geometric properties are found to propagate up to the final estimation of the oil film thickness and, consequently, the stiffness coefficient. Facing this problem, a statistical analysis of the experimental results is fundamental to establish a confidence bound of the parameters estimation. The confidence limits conditions were, then, numerically simulated and interesting results about the parameters sensitivity are reached. At this point, the experimental validation of the bearing model is presented in terms of mean value and standard deviation, considering Gaussian distribution for the uncertainties (Montgomery and Runger, 2011).

REVISION OF LITERATURE

The application of lubricated bearings in rotating machines with high operating speeds is specific critical due to the significant shearing of the fluid, substantially increasing the temperatures of the bearing and the fluid. Consequently, the viscosity of the fluid decreases, affecting the dynamic behavior of the bearing. Consequently, the influence of the thermal effects on the dynamic characteristics of the bearing must be taken into account, leading to the need of a thermohydrodynamic (THD) model for thrust bearings. According to Ahmed *et al.* (2010) "the few studies that can be found in the literature on thermal effects and deformations in hydrodynamic fixed geometry thrust bearings prove that the increase in the temperature has a great influence on thrust bearings characteristics".

Dowson (1962), presented the Generalized Reynolds' Equation used for the evaluation of the pressure distribution in the fluid, considering the variation of the fluid properties, such as viscosity and specific mass. Later, Dowson and March (1966), developed a THD analysis through the solution of the Generalized Reynolds' Equation and the Energy Equation applied to the fluid and the solid elements, obtaining good agreement with previous experimental results. At this point, the demand for reliable experimental results for comparison and validation of the numerical models increased. However, only at the 1990's, with the improvement of data acquisition and data processing systems, the experimental estimative of dynamic coefficients became more accessible.

For the specific case of thrust bearings, some recent works may be cited: Almqvist *et al.* (2000) compared the simulated results for a THD model to the experimental results obtained for a tilting pad thrust bearing. However, the simulations did not take into account the thermal effects on the fluid film. Glavatskih *et al.* (2002) used the same test bench to compare the results obtained with a Thermo-elasto-hydrodynamic (TEHD) model, with the objective of analyzing the influence of the lubricant fluid properties on the performance of the bearing.

Dadouche *et al.* (2000) experimentally investigated the influence of different operational conditions, as applied load, rotating speed and oil supply temperature, in a specific test bench for fixed geometry thrust bearing with large dimensions. The same test bench was used some years later by Dadouche *et al.* (2006) to compare experimental and simulation results, contributing to the development of the research and the state-of-the-art in the study of fixed geometry thrust bearings, less studied experimentally than the tilting pad bearings, according to the authors. Ahmed *et al.* (2010) also used the same test bench and compared the experimental results to those obtained by a TEHD model of the same thrust bearing, considering the deformation of the runner and of the bearings due to the pressure distribution within the fluid film.

The present work is placed in this historical context to present a THD analysis of fixed geometry thrust bearings using the Finite Volume Method to simultaneously solve the Generalized Reynolds' Equation and the Energy Equation, the evaluation of an equivalent stiffness of the oil film and its validation in a experimental and representative test rig, mainly to define the equilibrium position, namely, the oil film thickness in different rotation speeds and the uncertainties associated with the zero reference of the measurements and the axial clearance of the bearing. The experimental analysis of the thrust bearing was adapted to be accomplished in a small turbocharger at the TUD (Technische Universität Darmstadt), in Germany. The experiment concept elaboration also contributes to the state-of-the-art of the research and works as the initial step towards the development of a test bench with possibilities for analysis of high frequency and high loaded lubricated bearings.

PROBLEM DESCRIPTION

The evaluation of the equivalent coefficients of thrust bearings is not a simple task because it involves many parameters, such as axial clearance and film thickness. The problem investigated in this work is the influence of the uncertainties in the evaluation of the stiffness coefficient of the thrust bearing in a high speed automotive turbocharger.

Automotive turbochargers are used to improve the power of the internal combustion engine, increasing the air injected inside the combustion chamber. In the experimental test bench, compressed air is used to run the turbine and, consequently, the impeller causes axial forces in the rotating system, being necessary to use the thrust bearing to support them. Fig. 1 shows a simplified scheme of the system, indicating the shaft, the thrust and the radial bearings, the runner, the turbine and compressor rotors and the location of the position sensor.

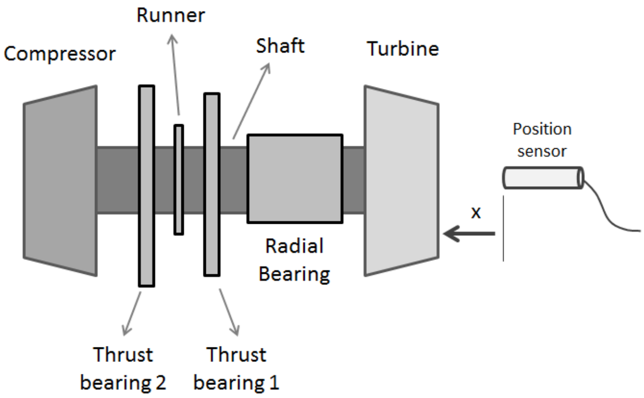

Figure 1 - Bearing assembly (out of scale).

The shaft, the runners, the turbine and the compressor may move axially and radially, while the bearings remain stationary. The axial movement is measured by the position sensor and has positive values towards the compressor, as indicated in Fig. 1.

In this system, axial clearance and film thickness represent critical parameters due to its influences in the equivalent coefficients of the thrust bearing. The axial clearance in the thrust bearing is measured using the position sensor, shifting the runner (rotor) from the thrust bearing 1 towards the thrust bearing 2. Consequently, this procedure presents uncertainties related to the assembly, manufacturing process and surfaces finishing, that certainly affects the evaluation of the equilibrium position of the shaft with respect to the bearing. It is important to clarify that the uncertainties associated to the instrumentation itself are not considered in the present analysis.

There is a second issue related to the measurements used to estimate the oil film thickness. The film thickness is measured taking the reference position at the thrust bearing 1, which means the relative distance of the runner (rotor) from the reference. Therefore, the reference position (x_0) occurs when the runner is in contact with the thrust bearing 1. Also in this case, the uncertainty in the reference position propagates to the measurements of the oil film thickness in the bearing. As previously mentioned, the uncertainties of these measurements certainly influence the evaluation of the equivalent stiffness coefficients, mainly due to its dependence on the equilibrium position of the runner at each rotation speed.

The uncertainties of the reference position (x_0) affect the film thickness (h), as described in the Eq. (1):

$$h = x - x_0 = K.V - x_0 \tag{1}$$

Where K is the sensor sensitivity (0.1604 mm/V) and V is the voltage acquired for each position.

The analysis here considers the surface of the runner as parallel to the surface of the bearing (Fig. 1) and neglects the existence of geometrical discontinuities in the materials. The stiffness coefficients were numerically estimated from the thermohydrodynamic lubrication model, in which the pressure distribution is obtained solving the Reynolds equation jointly with the energy equation. The Finite Volume Method is applied, according to the models described by Patankar (1980) and Arghir *et al.*(2002).

The Generalized Reynolds' Equation, introduced by Dowson (1962), is here adapted for the cylindrical coordinates, as follows:

$$\frac{1}{\mathrm{r}}\frac{\partial}{\partial\theta}\left(\mathrm{F}_2\frac{\partial \mathrm{p}}{\partial\theta}\right)+\frac{\partial}{\partial \mathrm{r}}\left(\mathrm{rF}_2\frac{\partial \mathrm{p}}{\partial \mathrm{r}}\right)=\omega \mathrm{r}\frac{\partial}{\partial\theta}\left[\frac{\mathrm{F}_1}{\mathrm{F}_0}\right]+\mathrm{r}\frac{\partial h}{\partial t} \tag{2}$$

where ω is the angular rotating speed of the shaft, *p* is the pressure generated within the fluid, h is the film thickness, *t* is the time, r and θ are the coordinates in the radial and angular directions, respectively, and the functions F_0, F_1 and F_2 are integrals responsible for coupling the variation of the temperature of the fluid and the fluid film pressure:

$$F_0=\int_0^{\mathrm{h}}\frac{1}{\mu}\mathrm{d}x \qquad F_1=\int_0^{\mathrm{h}}\frac{x}{\mu}\mathrm{d}x \qquad \mathrm{F}_2=\int_0^{h}\frac{\mathrm{x}}{\mu}\left(\mathrm{x}-\frac{\mathrm{F}_1}{\mathrm{F}_0}\right)d\mathrm{x} \tag{3}$$

being μ the absolute viscosity of the fluid and x the coordinate in the direction of the film thickness.

The Energy Equation considers all heat exchanges, due to conduction or convection, and the heat generated due to the viscous dissipation caused by the shearing of the fluid.

$$\rho C_p\left(u\frac{\partial T}{\partial x}+\frac{v_\theta}{r}\frac{\partial T}{\partial\theta}+v_r\frac{\partial T}{\partial r}\right)=k\frac{\partial^2 T}{\partial x^2}+k\frac{1}{r}\frac{\partial}{\partial r}\left(r\frac{\partial T}{\partial r}\right)+k\frac{1}{r^2}\frac{\partial^2 T}{\partial\theta^2}+\mu\Phi \tag{4}$$

where *T* is the fluid temperature, and *u*, *v* and *w* are the velocities of the fluid in the *x*, *y* and *z* directions, respectively, with $y=r*\cos(\theta)$ and $z=r*\sin(\theta)$. Still, ρ is the fluid's specific mass, *k* is its thermal conductivity, and C_p is the specific heat, all constant properties. The dissipative term is given by:

$$\Phi=\left(\frac{\partial v_r}{\partial x}\right)^2+\left(\frac{\partial v_\theta}{\partial x}\right)^2 \tag{5}$$

where v_r and v_θ are the fluid linear velocities in the radial and angular directions, respectively.

The equivalent stiffness coefficient is obtained by applying a small perturbation around the equilibrium position of the runner and taking into account the variation in the supported load, as suggested by Lund (1987). In this case, the Generalized Reynolds' Equation is evaluated considering an equilibrium position, what means that $\partial h/\partial t=0$ in Eq. (1). The ratio between the load variation (∂W_{total}) and the film thickness variation (∂x) results in the stiffness coefficient K_{xx}:

$$K_{xx} = \frac{\partial W_{\text{total}}}{\partial x} \tag{6}$$

EXPERIMENTAL PROCEDURE

Figure 2 shows a picture of the test bench used in the tests. It is possible to identify, in this figure, the oil and cool air supply systems, the cable of the position sensor, placed on the turbine side, and the system (strain gauges) used for measure the external axial force on the rotating shaft. The system works impelled by compressed air injected on the turbine side, causing the rotation of the shaft that connects the turbine to the compressor. The compressor side is open to allow the measurement of the rotating speed of the shaft. The lubricating oil is the Essolube© X2 20W oil, pumped from a reservoir. No specific oil cooling system is used. The inlet temperature in the thrust bearing is evaluated from the THD model of the radial bearings for each rotation speed, which means the inlet temperature in the thrust bearing is considerably higher than the oil temperature in the reservoir.

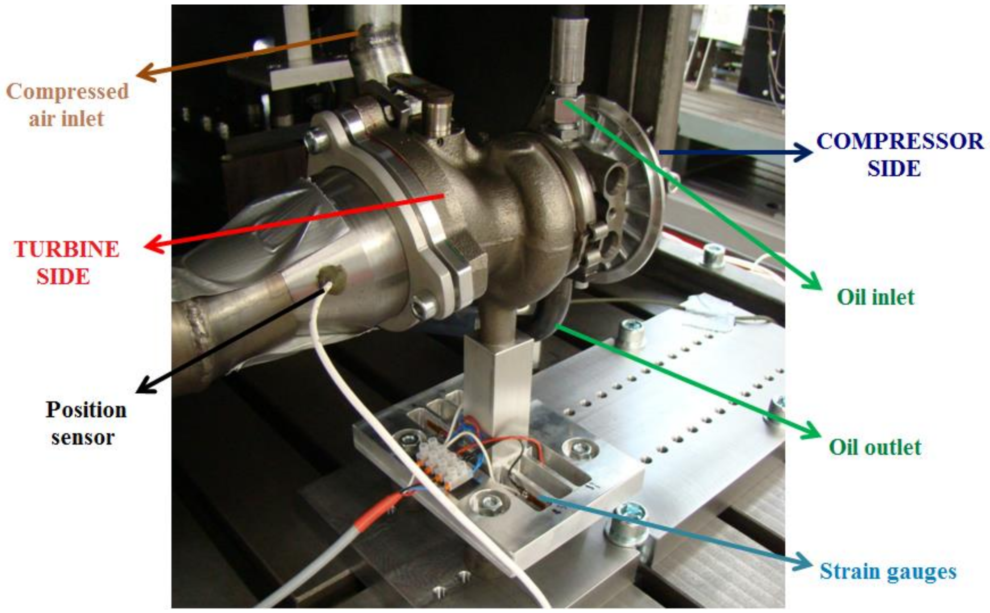

Figure 2 - Instrumented turbocompressor (TUD, Germany).

Two sensors were installed: one position sensor facing the shaft (in the axial direction) at the turbine side, as illustrated in Fig. 1; and one sensor for measuring the rotating speed of the shaft, installed at the compressor side. The position sensor aims to measure the axial displacement of the shaft, while the velocity sensor receives one pulse at each passage of one of the compressor blades. As the compressor has six blades, one rotation cycle is counted at every six pulses.

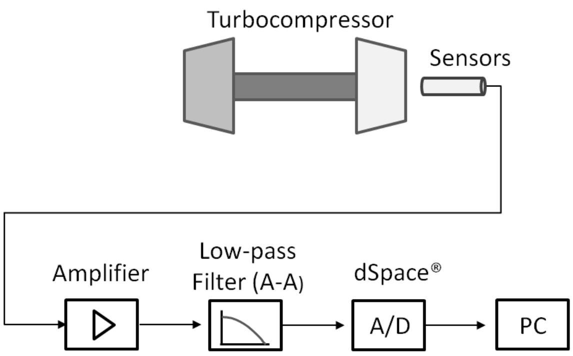

Figure 3 - Data acquisition system.

As shown in Fig. 3, the signal from the sensor passes through an amplifier and through a low-pass filter before being acquired by the dSpace© Digital/Analog filter. The position sensor – Fig. 4(a) - was calibrated with the reference (xo) obtained by axially moving the shaft until the runner touches the bearing 1, as shown in Fig. 4(b).

(a)

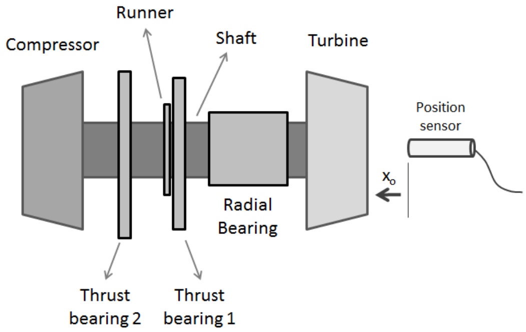

(b)

Figure 4 - Data acquisition system: (a) Position system; (b) Runner relative position at xo.

RESULTS

In order to verify the influence of uncertainties in the estimation of the stiffness coefficient of the thrust bearing assembled in a turbocharger, numerical simulations were accomplished considering different confidence intervals, such as $\mu \pm \sigma$, $\mu \pm 1.5 \cdot \sigma$ and $\mu \pm 2 \cdot \sigma$ where μ is the mean and σ is the standard deviation of the population. Regarding to axial clearance, the measurements obtained from the experimental tests provide $\mu = 45.5$ micrometer and $\sigma = 2.2$ micrometer.

The film thickness was obtained from the position sensor installed in the extremity of the turbocharger (see Fig. 4b). Thus, the uncertainties were considered in the reference position xo. The estimation of the mean and standard deviation of the reference position xo were based on the value measured in begging of the experiment with null rotation speed (mean value) and the standard deviation was assumed nearly 1% of the mean, resulting $\mu = 223.0$ micrometer and $\sigma = 2.2$ micrometer for the reference position xo. Tables 1-3 show the values of the parameters considered in each confidence interval.

Table 1 – Values of the parameters considering the confidence intervals $\mu \pm \sigma$

	$\bar{C} - \sigma_C$			$\bar{C}$			$\bar{C} + \sigma_C$		
	43.3			45.5			47.7		
	$\bar{x}_0 - \sigma_{x_0}$	$\bar{x}_0$	$\bar{x}_0 + \sigma_{x_0}$	$\bar{x}_0 - \sigma_{x_0}$	$\bar{x}_0$	$\bar{x}_0 + \sigma_{x_0}$	$\bar{x}_0 - \sigma_{x_0}$	$\bar{x}_0$	$\bar{x}_0 + \sigma_{x_0}$
	220.8	223.0	225.2	220.8	223.0	225.2	220.8	223.0	225.2
Ω	$x = f(\bar{x}_0 - \sigma_{x_0})$	$x = f(\bar{x}_0)$	$x = f(\bar{x}_0 + \sigma_{x_0})$	$x = f(\bar{x}_0 - \sigma_{x_0})$	$x = f(\bar{x}_0)$	$x = f(\bar{x}_0 + \sigma_{x_0})$	$x = f(\bar{x}_0 - \sigma_{x_0})$	$x = f(\bar{x}_0)$	$x = f(\bar{x}_0 + \sigma_{x_0})$
14100	21.6	19.3	17.1	21.6	19.3	17.1	21.6	19.3	17.1
20280	18.3	16.1	13.8	18.3	16.1	13.8	18.3	16.1	13.8
27580	15.0	12.8	10.6	15.0	12.8	10.6	15.0	12.8	10.6

According to the data in Tab. 1, computer simulations were carried out to verify the influence of uncertainties of the axial clearance and film thickness in the determination of the stiffness coefficient in the thrust bearing, considering a confidence interval of 68.26% within $\mu \pm \sigma$.

As can be verified in Fig. 5, the influence of the film thickness is more significant than the influence of axial clearance. This behavior can be observed by comparing Figs. 5 (a-c) to Figs. 5 (d-f). Furthermore, it is possible to verify that the equivalent stiffness coefficient obtained numerically tends to approach to the experimental result as the film thickness increases, i.e. the reference position decreases (see Eq.(1)). However, although the variations in film thickness tend to reduce the difference between the numerical and experimental results, the equivalent stiffness coefficient obtained experimentally in the thrust bearing is still outside the confidence interval.

Table 2 – Values of the parameters considering the confidence intervals $\mu \pm 1.5 \cdot \sigma$

	$\bar{C}-1.5\sigma_C$			$\bar{C}$			$\bar{C}+1.5\sigma_C$		
	42.2			45.5			48.8		
	$\bar{x}_0-1.5\sigma_{x_0}$	$\bar{x}_0$	$\bar{x}_0+1.5\sigma_{x_0}$	$\bar{x}_0-1.5\sigma_{x_0}$	$\bar{x}_0$	$\bar{x}_0+1.5\sigma_{x_0}$	$\bar{x}_0-1.5\sigma_{x_0}$	$\bar{x}_0$	$\bar{x}_0+1.5\sigma_{x_0}$
	219.7	223.0	226.3	219.7	223.0	226.3	219.7	223.0	226.3
Ω	$x = f(\bar{x}_0-1.5\sigma_{x_0})$	$x = f(\bar{x}_0)$	$x = f(\bar{x}_0+1.5\sigma_{x_0})$	$x = f(\bar{x}_0-1.5\sigma_{x_0})$	$x = f(\bar{x}_0)$	$x = f(\bar{x}_0+1.5\sigma_{x_0})$	$x = f(\bar{x}_0-1.5\sigma_{x_0})$	$x = f(\bar{x}_0)$	$x = f(\bar{x}_0+1.5\sigma_{x_0})$
14100	22.7	19.3	16.0	22.7	19.3	16.0	22.7	19.3	16.0
20280	19.4	16.1	12.7	19.4	16.1	12.7	19.4	16.1	12.7
27580	16.1	12.8	9.4	16.1	12.8	9.4	16.1	12.8	9.4

Table 3 – Values of the parameters considering the confidence intervals $\mu \pm 2.0 \cdot \sigma$

	$\bar{C}-2\sigma_C$			$\bar{C}$			$\bar{C}+2\sigma_C$		
	41.1			45.5			49.9		
	$\bar{x}_0-2\sigma_{x_0}$	$\bar{x}_0$	$\bar{x}_0+2\sigma_{x_0}$	$\bar{x}_0-2\sigma_{x_0}$	$\bar{x}_0$	$\bar{x}_0+2\sigma_{x_0}$	$\bar{x}_0-2\sigma_{x_0}$	$\bar{x}_0$	$\bar{x}_0+2\sigma_{x_0}$
	218.5	223.0	227.5	218.5	223.0	227.5	218.5	223.0	227.5
Ω	$x = f(\bar{x}_0-2\sigma_{x_0})$	$x = f(\bar{x}_0)$	$x = f(\bar{x}_0+2\sigma_{x_0})$	$x = f(\bar{x}_0-2\sigma_{x_0})$	$x = f(\bar{x}_0)$	$x = f(\bar{x}_0+2\sigma_{x_0})$	$x = f(\bar{x}_0-2\sigma_{x_0})$	$x = f(\bar{x}_0)$	$x = f(\bar{x}_0+2\sigma_{x_0})$
14100	23.8	19.3	14.9	23.8	19.3	14.9	23.8	19.3	14.9
20280	20.5	16.1	11.6	20.5	16.1	11.6	20.5	16.1	11.6
27580	17.2	12.8	8.3	17.2	12.8	8.3	17.2	12.8	8.3

Therefore, numerical simulations were performed considering a confidence interval $\mu \pm 1.5 \cdot \sigma$, namely, 86,64%, aiming to ensure that the experimental result is inserted into the confidence interval.

The data used in the numerical simulations for the confidence interval $\mu \pm 1.5 \cdot \sigma$ were presented in the Tab. 2. It is important to highlight that the confidence interval $\mu \pm 1.5 \cdot \sigma$ as considered for both parameter (axial clearance and reference position).

Figure 6 shows the equivalent stiffness coefficient considering the confidence interval $\mu \pm 1.5 \cdot \sigma$. Also in this case, the influence of the film thickness is more significant than the influence of axial clearance, as can be observed by comparing Figs. 6 (a-c) to Figs. 6 (d-f). However, although the influence of the parameters maintains the previous tendency, the equivalent stiffness coefficient tends to approach to the experimental result as both parameters increase, respectively, axial clearance and film thickness. In this case, the lowest difference between the numerical and experimental results is obtained when considering the maximum axial clearance and the minimum reference position, as observed in Fig. 6(c). However, a good approach can be observed in the comparison of numerical end experimental results, and the tendency of the curves is quite similar.

Finally, the confidence interval was taken at 95.44% and numerical simulations were also accomplished considering the data obtained from the interval $\mu \pm 2 \cdot \sigma$. The data used in these numerical simulations are showed in Tab. 3.

Figure 7 shows the equivalent stiffness coefficient of the thrust bearing for the confidence interval $\mu \pm 2 \cdot \sigma$. As previously described, the influence of the film thickness is more significant than the influence of the axial clearance, as can be observed by comparing Figs. 7 (a-c) to Figs. 7 (d-f). Also in this case, the lowest difference between the numerical and experimental results occurs with maximum axial clearance and minimum reference position. Finally, in this case, the equivalent stiffness coefficient obtained numerically is in very good agreement to the equivalent stiffness coefficient obtained experimentally, as can be observed in Fig. 7(c).

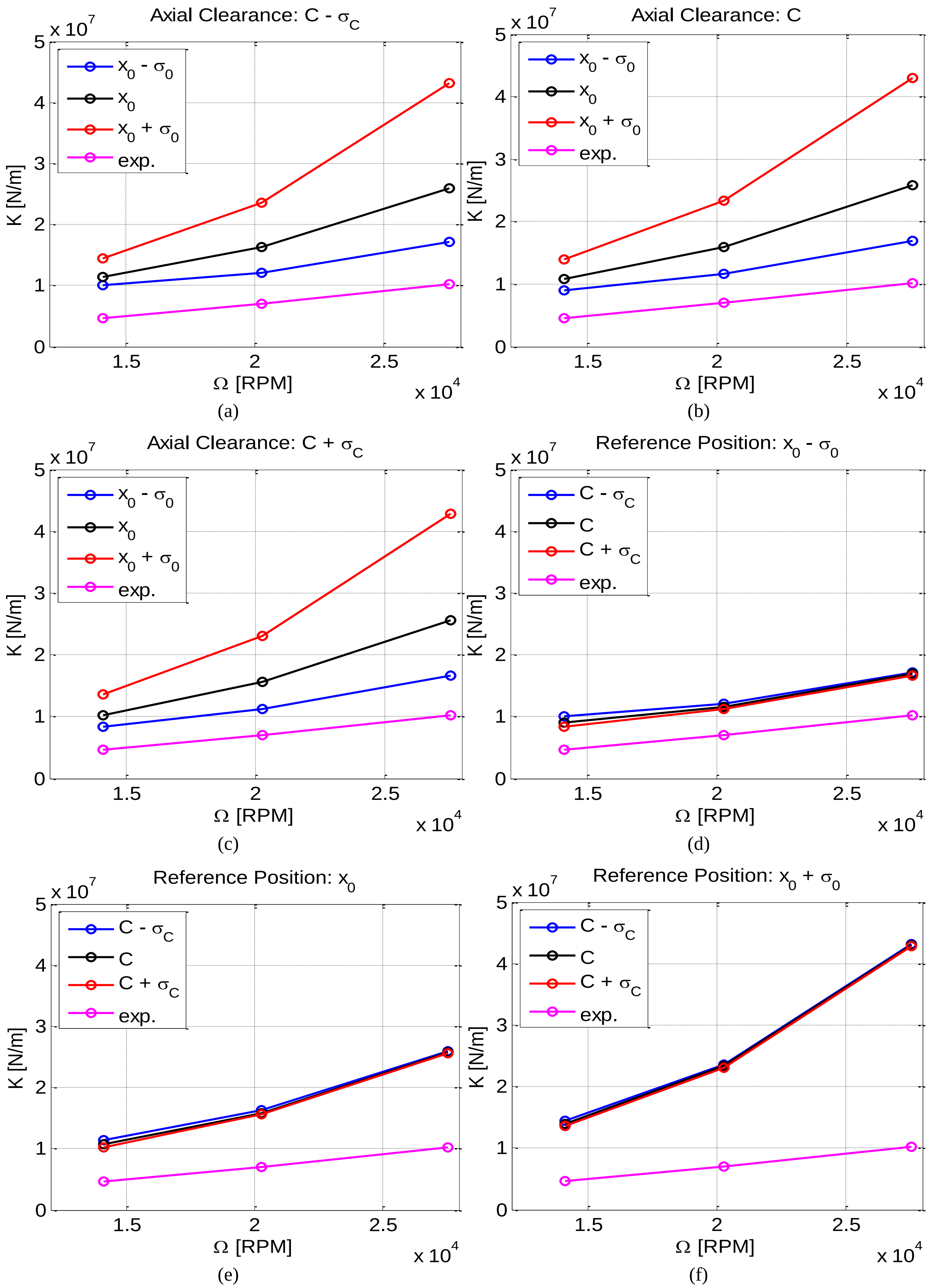

Figure 5 – Stiffness coefficient of the thrust bearing considering the confidence interval of $\mu \pm \sigma$. (a), (b) and (c) Influence of the reference positon in the stiffness coefficient for the minimum, medium and maximum axial clearance, respectively. (d), (e) and (f) Influence of the axial clearance in the stiffness coefficient for the minimum, medium and maximum reference positon, respectively.

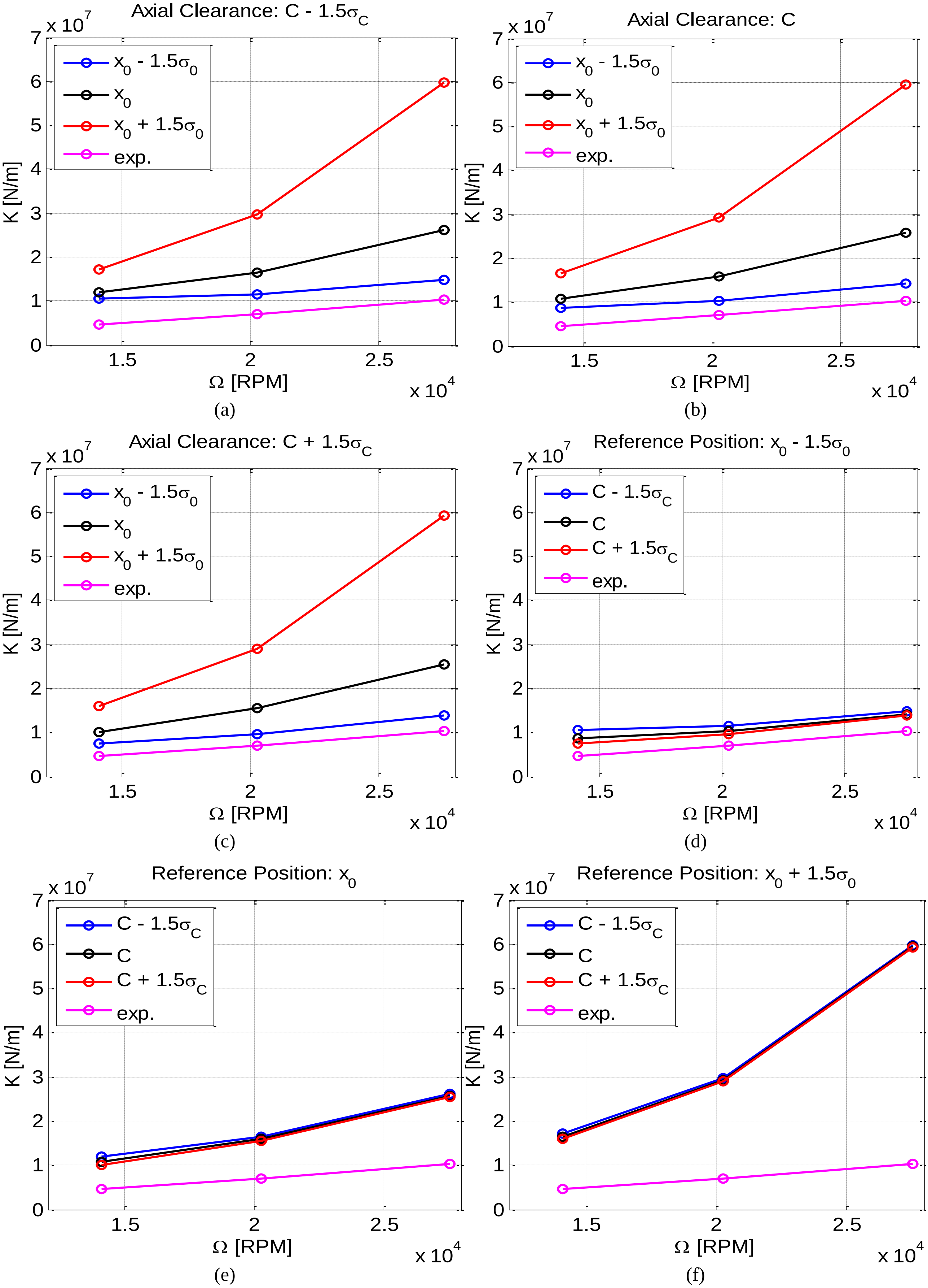

Figure 6 – Stiffness coefficient of the thrust bearing considering the confidence interval of $\mu \pm 1.5\sigma$. (a), (b) and (c) Influence of the reference positon in the stiffness coefficient for the minimum, medium and maximum axial clearance, respectively. (d), (e) and (f) Influence of the axial clearance in the stiffness coefficient for the minimum, medium and maximum reference positon, respectively.

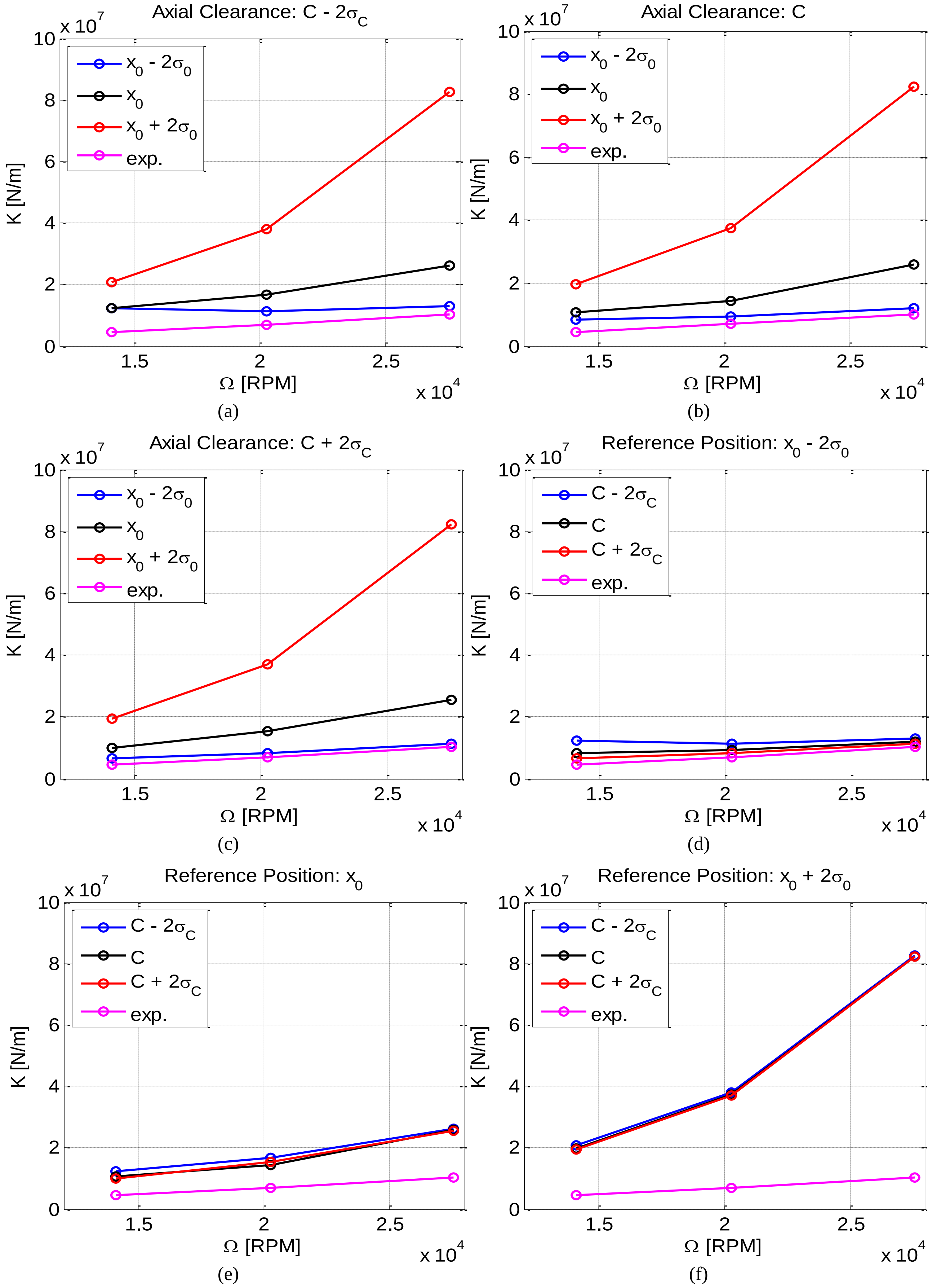

Figure 7 – Stiffness coefficient of the thrust bearing considering the confidence interval of $\mu \pm 2\sigma$. (a), (b) and (c) Influence of the reference positon in the stiffness coefficient for the minimum, medium and maximum axial clearance, respectively. (d), (e) and (f) Influence of the axial clearance in the stiffness coefficient for the minimum, medium and maximum reference positon, respectively.

CONCLUSIONS

The main purpose of this work is to validate the axial stiffness coefficient of a hydrodynamic thrust bearings and its dependence on the rotation speed, taking into account thermal effects on the numerical model. An experimental test bench was adapted to obtain the measurements related to the equilibrium position of the shaft at each rotation speed. This parameter is essential to evaluate the stiffness coefficient. However, it depends on crucial physical measures of axial clearance and the position sensor reference system (the zero point). Both measures involve uncertainties that propagate and affect the evaluation of the coefficient. At this point, the uncertainties influence was investigated for three confidence intervals, namely, 68.26%, 86.64% and 95.44%.

The sensitivity analysis shows that the oil film thickness (or the reference position) has more expressive influence on the results than the axial clearance.

The most promising combination of those physical measures boundaries was the maximum axial clearance and the minimum reference position to the sensor, or the maximum oil film thickness.

The numerical approach can be considered promising and in good agreement with the experimental results when considering confidence levels of 86.64% and 95.44%.

However, the main point to be highlighted here is when dealing with complex experiments involving variability due to assembling or even manufacturing, a model validation based on the uncertainties propagation influence is crucial.

ACKNOWLEDGMENTS

The authors would like to thank CAPES-PROBRAL, CNPq and BorgWarner Brasil Ldta for the financial support of this research. Special acknowledgements to Prof. Richard Markert from TU Darmstadt for kindly facilitate the use and adaptation of the experimental test rig.

REFERENCES

Ahmed S.A., Fillon M., Maspeyrot P., 2010, "Influence of Pad and Runner Mechanical Deformations on the Performance of a Hydrodynamic Fixed Geometry Thrust Bearing", Proc. of the Institution of Mechanical Engineers, Part J: Journal of Engineering Tribology, n. 224, pp.305-315.

Almqvist T., Glavatskih S.B., Larsson R., 2000, "THD Analysis of Tilting Pad Thrust Bearings - Comparison Between Theory and Experiments", Transactions of the ASME, n.122, pp.122-417.

Arghir M., Alsayed A., Nicolas D., 2002, "The Finite Volume Solution of the Reynolds Equation of Lubrication with Film Discontinuities", International Journal of Mechanical Sciences, v.44, pp.2119-2132.

Dadouche A., Fillon M., Bligoud J., 2000, "Experiments on Thermal Effects in a Hydrodynamic Thrust Bearing", *Tribology International*, n.33, pp.167-174.

Dadouche A., Fillon M., Dmochowski W., 2006, "Performance of a Hydrodynamic Fixed Geometry Thrust Bearing: Comparison between Experimental Data and Numerical Results", Tribology Transactions, n.49, pp.419-426.

Dowson D., 1962, "A Generalized Reynolds Equation for Fluid Film Lubrication", International Journal of Mechanical Sciences, n.4, pp.159-170.

Dowson D., March C., 1966, "A Thermohydrodynamic Analysis of Journal Bearings", Proc. of the Institution of Mechanical Engineers, n.181, pp.117-126.

Glavatskih S.B., Fillon M., Larsson R., 2002 "The Significance of Oil Thermal Properties on the Performance of a Tilting-Pad Thrust Bearing", Journal of Tribology, n.124, pp.377-385.

Montgomery D.C., and Runger G.C., 2011, "Applied Statistics and Probability for Engineers", Ed. John Wiley and Sons Inc., USA, 768 p.

Patankar S.V., 1980, "Numerical Heat Transfer and Fluid Flow", Hemisphere Publishing Corporation, McGraw-Hill Book Company, Washington DC, 197p.

RESPONSIBILITY NOTICE

The authors are the only responsible for the material included in this paper.